Deuterium excess in marine water vapor: Dependency on relative humidity and surface wind speed during evaporation

Marion Benetti, Gilles Reverdin, Catherine Pierre, Liliane Merlivat, Camille Risi, Hans Christian Steen-Larsen, Françoise Vimeux

AGU PUBLICATIONS

JGR

Journal of Geophysical Research: Atmospheres

RESEARCH ARTICLE
10.1002/2013JD020535

Key Points:
- Deuterium excess in low-level water vapor is mainly controlled by humidity
- Deuterium excess presents no clear influence of mixing processes
- Molecular diffusivities from Merlivat [1978a] are in agreement with the data

Correspondence to:
M. Benetti,
marionbenetti@locean-ipsl.upmc.fr

Citation:
Benetti, M., G. Reverdin, C. Pierre, L. Merlivat, C. Risi, H. C. Steen-Larsen, and F. Vimeux (2014), Deuterium excess in marine water vapor: Dependency on relative humidity and surface wind speed during evaporation, *J. Geophys. Res. Atmos.*, *119*, 584–593, doi:10.1002/2013JD020535.

Received 9 JUL 2013
Accepted 30 DEC 2013
Accepted article online 5 JAN 2014
Published online 29 JAN 2014

Deuterium excess in marine water vapor: Dependency on relative humidity and surface wind speed during evaporation

Marion Benetti[1], Gilles Reverdin[1], Catherine Pierre[1], Liliane Merlivat[1], Camille Risi[2], Hans Christian Steen-Larsen[3], and Françoise Vimeux[3,4]

[1]Laboratoire d'Océanographie et du Climat, Expérimentations et approches Numériques, IPSL, UPMC, CNRS, Paris, France, [2]Laboratoire de Météorologie Dynamique, IPSL, UPMC, CNRS, Paris, France, [3]Laboratoire des Sciences du Climat et de l'Environnement, CEA Saclay, Gif-sur-Yvette, France, [4]Laboratoire HydroSciences, IRD, Montpellier, France

Abstract We provide the first continuous measurements of isotopic composition (δD and δ^{18}O) of water vapor over the subtropical Eastern North Atlantic Ocean from mid-August to mid-September 2012. The ship was located mostly around 26°N, 35°W where evaporation exceeded by far precipitation and water vapor at 20 m largely originated from surface evaporation. The only large deviations from that occurred during a 2 day period in the vicinity of a weak low-pressure system. The continuous measurements were used to investigate deuterium excess (d-excess) relation to evaporation. During 25 days d-excess was negatively correlated with relative humidity ($r^2 = 0.89$). Moreover, d-excess estimated in an evaporative model with a closure assumption reproduced most of the observed variability. From these observations, the d-excess parameter seems to be a good indicator of evaporative conditions. We also conclude that in this region, d-excess into the marine boundary layer is less affected by mixing with the free troposphere than the isotopic composition. From our data, the transition from smooth to rough regime at the ocean surface is associated with a d-excess decrease of 5‰, which suggests the importance of the ocean surface roughness in controlling d-excess in this region.

1. Introduction

Continuous measurements of stable isotopic composition of water vapor (δ^{18}O and δD) have only recently become feasible with laser spectrometry, thus contributing to improve our understanding of the water cycle and of its effects on isotopic composition of water vapor. Ocean evaporation is the first phase change in the water cycle and leads to water vapor largely depleted in heavy isotopes compared to sea surface water. The deuterium excess (d-excess) (δD-8δ^{18}O) in newly evaporated water vapor results from a kinetic process [*Dansgaard*, 1964] which is controlled by evaporative conditions combining sea surface temperature, relative humidity, and wind speed [e.g., *Merlivat and Jouzel*, 1979 (MJ79); *Gat*, 1996; *Gat et al*., 2003; *Uemura et al*., 2008]. To date, few isotopic data of water vapor are available above the ocean [e.g., *Lawrence et al*., 2004; *Uemura et al*., 2008; *Kurita*, 2011, 2013; *Kurita et al*., 2011]. Here we provide a continuous measurement of the newly evaporated vapor with simultaneous high temporal resolution of wind speed. During the STRASSE expedition (subtropical Atlantic surface salinity experiment), the ship (RV *Thalassa*) stayed in the North Atlantic subtropical region of high excess evaporation [*Wüst*, 1922] mostly around 26°N, 35°W from mid-August to mid-September 2012 (Figure 1).

The wind direction was mainly from the east corresponding to trade winds. Moreover, convective processes and precipitation events are not common during this season, which is usually characterized by large-scale dry air subsidence. Radiosondes indicate that the relative humidity of the lower troposphere was particularly dry, mostly around 40% above the planetary boundary layer (PBL); except for a 2 day event around the 1 September where relative humidity reached 90% in the lower atmosphere. This short event, associated with vertical convection, reflects unstable atmospheric conditions that were not encountered at other times. Because of the weak convection and dry troposphere, most of the time, the water vapor in the PBL was not much affected by the water vapor above the PBL. Consequently, the cruise atmospheric conditions are favorable to explore characteristics of the water vapor mainly influenced by evaporation processes at the ocean surface. In this study we present the data set and check the hypothesis of local evaporation imprinting

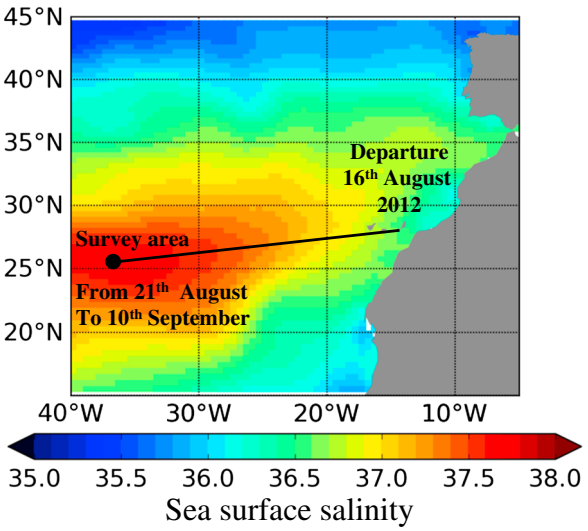

Figure 1. Trajectory of the ship during the STRASSE cruise. The ship left the Canary Islands on 16 August and arrived 5 days later in the survey area around 26°N, 35°W where it stayed 3 weeks. The survey area in the NE Atlantic corresponds to the region of salinity maximum (37.75‰) where evaporation exceeds largely precipitation in this season (the salinity map is from ISAS (In Situ Analysis System) objective analysis of Argo profile data for August 2012). The ISAS method is described in *Gaillard et al*. [2009].

d-excess of the near surface water vapor. We examine the d-excess dependency on relative humidity with respect to the sea surface temperature (Rhs) and wind speed. A better understanding of the link between these three parameters is important because d-excess is used as a proxy for moisture source conditions in paleoclimatology [e.g., *Jouzel et al.*, 1982]. We will compare observed d-excess with d-excess estimated by a closure assumption (MJ79). The closure equation established by MJ79 assumes that the water vapor in the PBL originates only from ocean evaporation and is not influenced by other atmospheric processes. The relevance of this assumption will be checked. Moreover, the high temporal resolution of the measurements will be used to check the kinetic fractionation factors proposed by MJ79 that depend among others on surface roughness.

2. Measurements and Atmospheric Conditions

2.1. Isotopes in Water Vapor

A laser analyzer Picarro L2130-i equipment was installed on the top deck of RV *Thalassa* with air pumped at an altitude of 20 m above the sea surface, just under the meteorological station. We used a 10 m long perfluoroalkoxy (PFA) tube and a 6 L/min extra pump to carry water vapor from the collecting site to the analyzer. PFA tubing has been chosen because of its weak concentration dependent and memory effect [*Schmidt et al.*, 2010; *Tremoy et al.*, 2011]. The PFA tube was permanently heated at 40°C to avoid postcondensation processes. For the calibration, we followed the protocol elaborated by [*Steen-Larsen et al.*, 2013]. Dry air was used during liquid water calibrations, to be as close as possible to the water vapor measurement conditions. Because we did not have the Standards Delivery Module (Picarro) system or equivalent, the liquid injections were done with an autosampler. As recommended by *Schmidt et al.* [2010], *Tremoy et al.* [2011], and *Steen-Larsen et al.* [2013], we tested the dependency of the measured isotopic values on the water concentration with liquid samples. The liquid samples have isotopic compositions close to the δ values of the vapor measurements during the cruise ($\delta^{18}O = -15.81‰$ Vienna standard mean ocean water (V-SMOW); $\delta^{2}H = -120.68‰$ V-SMOW). Two tests have been done in field conditions, one in the middle (29 August) and another at the end of the cruise (13 September) and showed the same trend with a $\delta^{18}O$ increase of 0.15‰ and a $\delta^{2}H$ decrease of 0.3‰ between a water concentration of 20 000 and one of 34 000 ppmv (Figure 2). Both tests were done by injecting different amounts of liquid water into the vaporizer thereby creating different humidity concentrations. During the cruise vapor measurements, we obtained a precision of 0.16‰ for $\delta^{18}O$, 0.4‰ for δD, and 1.4‰ for d-excess. Compared to instrumental precision, the concentration effect is slightly significant for $\delta^{18}O$ and insignificant for δD. We found that the measurements with water concentration up to specification from Picarro ($>$30 000 ppmv) are working well. To correct the raw data from the concentration effect, we chose 20 000 ppmv humidity level as reference, as done in other studies [*Tremoy et al.*, 2011; *Steen-Larsen et al.*, 2013].

The temperature inside the Picarro's room varied between 20 and 30°C, mostly influenced by the wind strength and the diurnal cycle. The ambient temperature inside the Picarro was observed to have fluctuations lower than 10°C during the cruise. During this cruise, no correlation was observed between the temperature inside the Picarro and isotopic measurements. We did not observe any temperature effect on our measurements with the L2130-I model. The drift of the instrument was measured by injecting a liquid reference 10 consecutive times every 6 h during the first 2 weeks (see results Figure 3). Later on we reduced by a factor of 2

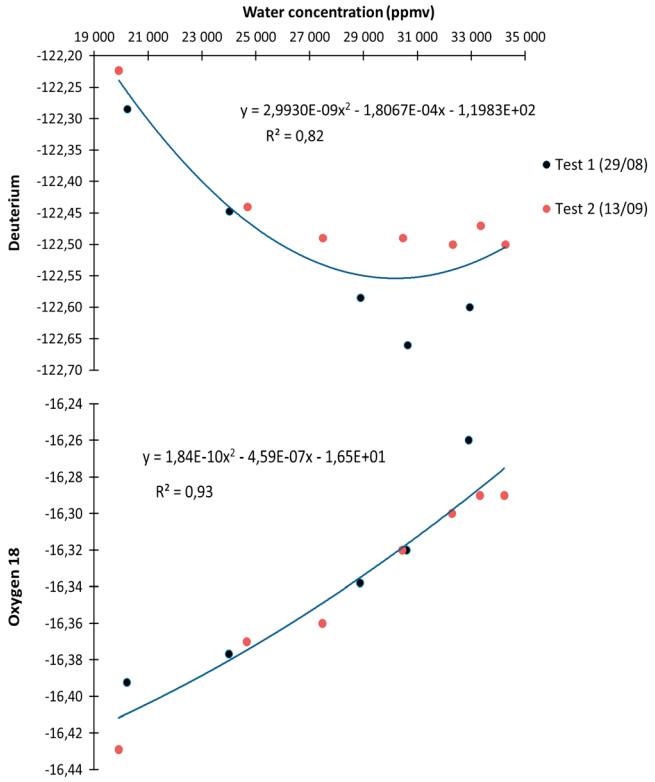

Figure 2. Isotopic composition measured by Picarro L2130-i resulting from injections of water concentration from 20,000 to 30,000 ppmv. The drift between the 19 August and the 13 September has been corrected. The last three of six injections were averaged. Standard deviations are lower than 0.05‰ for $\delta^{18}O$ and 0.5‰ for δD. Curves show the regressions for all measurements (Test 1 and Test 2).

the reference injections, as the system proved to be very stable. The liquid reference used had an isotopic composition close to the water vapor measured. During the month of measurement, the drift for $\delta^{18}O$ was 0.3‰ (see Figure 3). The standard deviation of $\delta^{18}O$ is based on repetitive experiments with this instrument and was small with a value of 0.05‰. We chose not to correct the drift effect in δD measurements, because the accuracy of the δD measurement was comparable to the drift. To transfer the measurement in the instrument scale to the V-SMOW scale, three liquid references with known isotopic compositions ($\delta^{18}O$, δD; −0.56‰ V-SMOW, −3.75‰ V-SMOW; −6.60‰ V-SMOW, −45.42‰ V-SMOW; −15.81‰ V-SMOW, −120.68‰ V-SMOW) were measured 5 times at 20 000 ppmv humidity level (reference level). The five calibrations show a high stability of the slope ($\delta^{18}O$: 0.991 ± 0.003 and δD: 0.977 ± 0.002), with negligible variations in time.

2.2. Isotopes in Sea Water

The sea surface water was also regularly collected (3 times a day at 3 m depth). Surface salinity, based on measurements from a calibrated Thermosalinograph, did not vary much during the survey (from 36.3 (coastal ocean) to 37.75‰ (survey area)). As a result, only 26 samples have been analyzed in laboratory (Laboratory for Oceanography and Climate: Experiments and Numerical Approaches (LOCEAN)) with an accuracy of 0.05‰ for $\delta^{18}O$ and 0.3‰ for δD. All samples have been distilled to avoid salt accumulation in the vaporizer. From several laboratory tests, the uncertainty due to the distillation is inferior to the accuracy of the Picarro L2130-i measurement. Figure 4 shows the isotopic composition of surface sea water during the cruise. The $\delta^{18}O$ (δD) varied from 1.02 (6.6) to 1.34 (9.0)‰.

2.3. Atmospheric Conditions

A meteorological station Batos from the French Met Office was located close to where the air was pumped. It measured continuously relative humidity (RH), air temperature (Ta), wind speed, and direction of wind

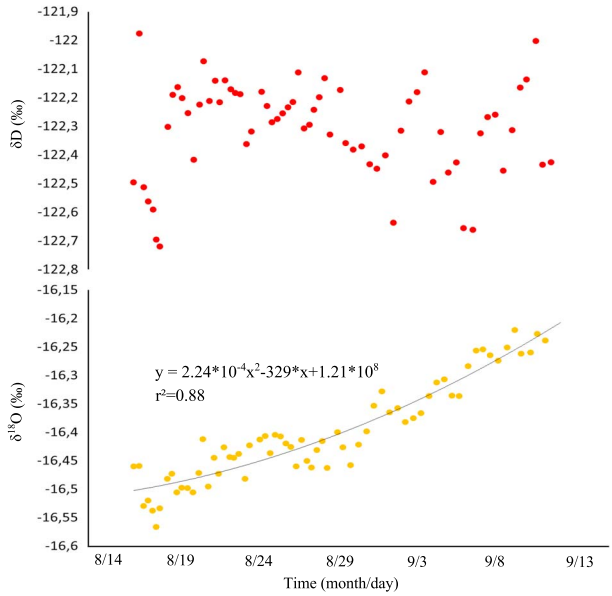

Figure 3. Drift of the Picarro L2130-I during the month of measurement. The accuracy is 0.05‰ for δ^{18}O and 0.3‰ for δD. The drift for δ^{18}O was 0.3‰. We chose not to correct the drift effect in δD measurements, because the accuracy of the δ^{2}H measurement is comparable to the drift.

(measurement every 30 s). The evolution of the main atmospheric parameters is presented in Figure 5. During the cruise we encountered a range of RH variation from 65 to 90%. RH was checked against readings of a psychrometer, and other parameters (temperature, wind speed, and wind direction) were compared with data from another automated station placed on a dedicated mast near the bow of the ship. The largest uncertainties are in RH that might differ at times by 2%. During the survey Ta was around 26°C with a diurnal cycle of 0.5°C, whereas close to the Canary Islands, Ta was 4°C lower. At the beginning of the cruise the wind was from the north. During the survey wind direction was mainly from the east, except during a 2 day event around the 1 September when the wind became northerly (red shading in Figures 5 and 8). Radiosondes have been launched during a part of the survey (morning and evening from 28 August to 09 September) and show a boundary layer thickness close to 1 km before 30 August and of almost 2 km after 2 September (see Figure 6). The variations of the isotopic composition of the water vapor (see Figure 5) were weak, and the isotopic composition was mostly between −9.5‰ (−70‰) and −11‰ (−80‰) for δ^{18}O (δD). These values are typical of the evaporated water vapor above the subtropical ocean [*Craig and Gordon*, 1965]. The δD of the water vapor in the subtropical western Pacific is mainly between −75‰ and −90‰ with extreme negative values reaching

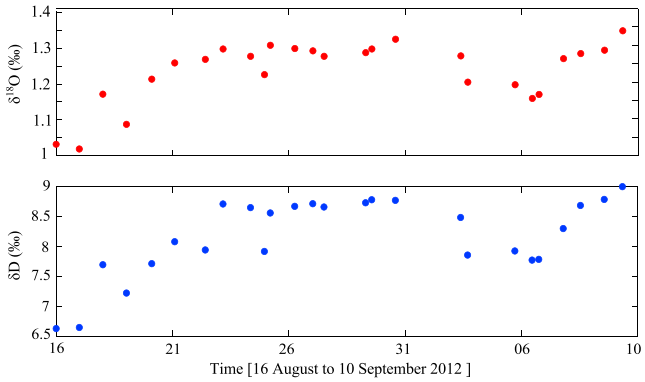

Figure 4. Isotopic composition of the 26 surface sea water samples during the cruise. The red and blue points are, respectively, measurements for δ^{18}O and δD. The sampling depth is 3 m below the sea surface. All the samples were analyzed in laboratory LOCEAN with an accuracy of 0.05‰ for δ^{18}O and 0.3‰ for δD.

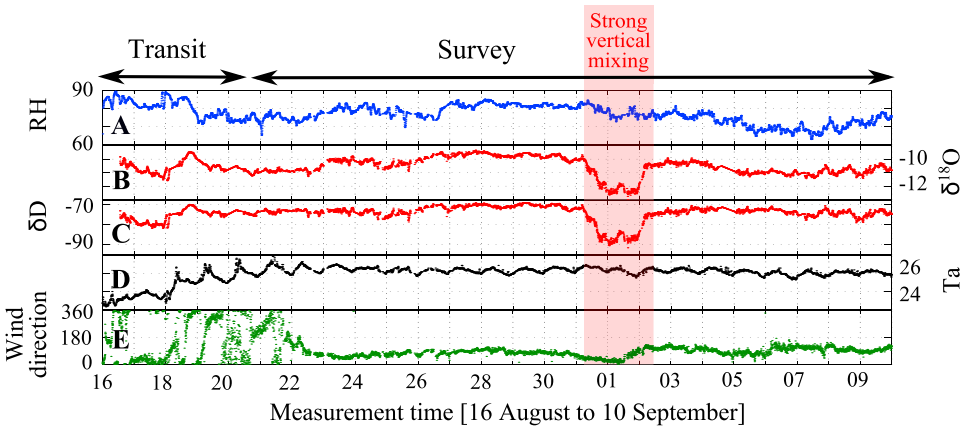

Figure 5. Evolution versus time of (a) relative humidity (%), (b) δ^{18}O (‰), (c) δ^{2}H (‰), (d) air temperature (degrees celsius), and (e) wind direction (0° for northerly wind and 180° for southerly wind) during the STRASSE cruise. The red shading period corresponds to important vertical mixing with the lower troposphere as diagnosed by radiosondages.

−110‰ [*Kurita*, 2013]. Nevertheless, we note in our data a short period of decrease (2.5‰ for δ^{18}O and 18‰ for δ^{2}H) around the 1 September corresponding to a vapor depleted during convective processes. At this time, cumulonimbus clouds and one precipitation event were observed from the ship. From observations in the tropics, *Lawrence et al.* [2004] and *Tremoy et al.* [2012] documented the effects of convective activity on the isotopic composition: strong convective activity leads to depleted water vapor. This relation is due to the "amount effect" demonstrated by a negative correlation between the amount of precipitation and their isotopic composition [*Dansgaard*, 1964]. This mechanism affects the subsequent water vapor.

3. Results and Discussion

3.1. The Closure Equation

In this area of high excess evaporation we compare our data with the d-excess estimated by the closure equation (1). Assuming that there is no other water vapor source than the sea surface, the isotopic composition of the PBL equals the isotopic composition of the net evaporated flux leading to the following equation (MJ79):

$$R_{BL} = \frac{R_{SW}}{\alpha_{eq}(\alpha_k + \mathrm{Rhs}(1-\alpha_k))} \quad (1)$$

where α_{eq} and α_k are the equilibrium and kinetic fractionation factors, R_{sw} is the isotopic ratio of seawater. The isotopic compositions of seawater are extrapolated (nearest neighbor extrapolation) from 26 sea surface samples (see Figure 4). The values of the isotopic composition of surface seawater vary from 1.02‰ (6.6‰) (coastal region) to 1.34‰ (9‰) (survey area) for δ^{18}O (δD) (see Figure 4). α_{eq} is based on experimental results from *Majoube* [1971] and is in agreement with more recent experimental results [e.g., *Horita and Wesolowski*, 1994; *Barkan and Luz*, 2005]. α_k depends on the ocean surface roughness (thus on the wind speed) and on molecular diffusivities (D_i) in air for each isotopic molecule. To date, there is a disagreement on the estimation of D_i [e.g., *Merlivat*, 1978; *Cappa et al.*, 2003; *Luz et al.*, 2009]. Estimations from *Cappa et al.* [2003] are significantly different from the two other studies, which present a close agreement. Here our calculations use D_i from *Merlivat* [1978] (but D_i from Cappa's estimations will also be briefly discussed). We used two constant values of α_k for the two regimes. Thus, when the wind speed at 10 m is larger than 7 m s^{-1}, corresponding to a rough regime, we use $\alpha_k{}^{18}\mathrm{O} = 1.0035$ and $\alpha_k\mathrm{D} = 1.0031$. Otherwise during the smooth regime, we use larger kinetic factors: $\alpha_k{}^{18}\mathrm{O} = 1.0060$ and $\alpha_k\mathrm{D} = 1.0053$ (MJ79). Rhs is the relative humidity with respect to the sea surface temperature (equation (2)).

$$\mathrm{Rhs} = \mathrm{Rha}.\frac{q_{sat}(\mathrm{Ta})}{q_{sat}(\mathrm{SST})} \quad (2)$$

Rha is the relative humidity of the near-surface air and q_{sat} is the specific humidity at saturation. Ta is the air temperature and SST is the sea surface temperature.

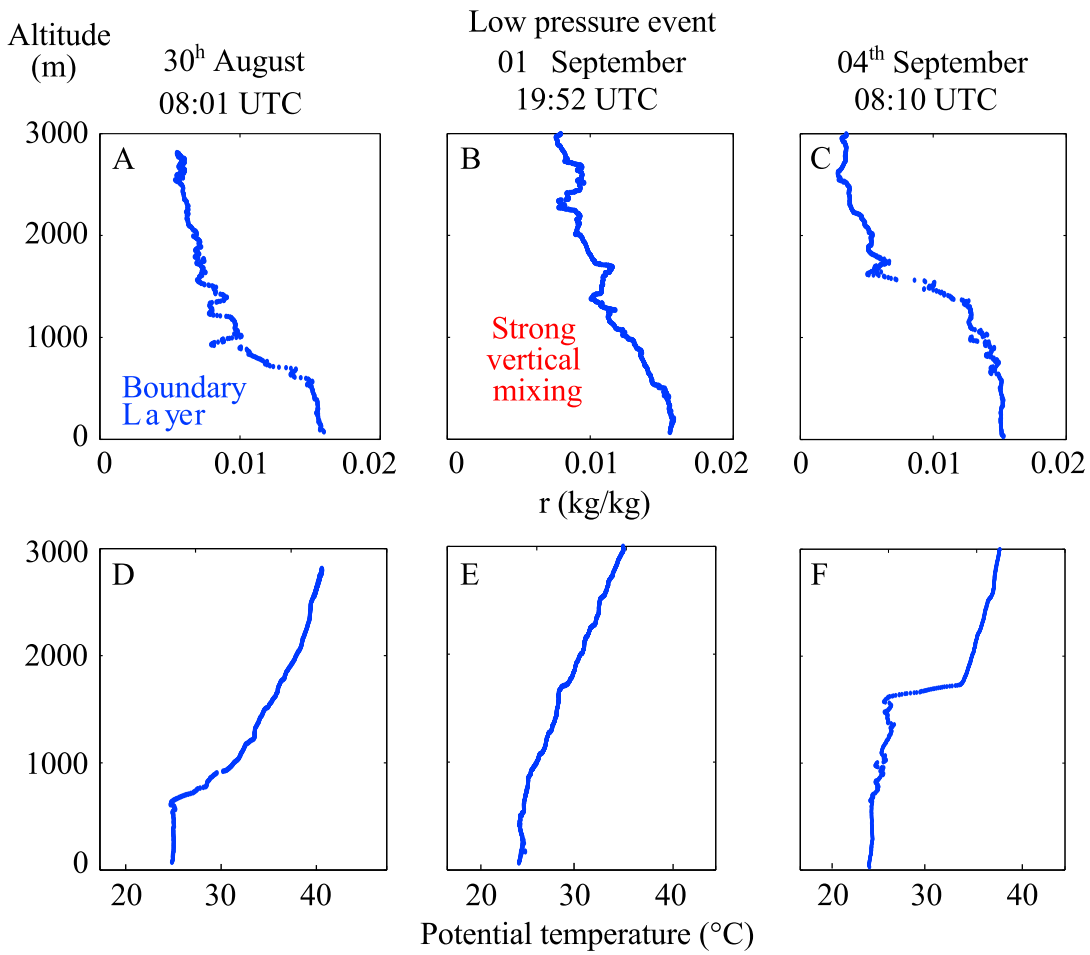

Figure 6. Vertical profiles of mixing ratio (a) before, (b) during, and (c) after the passage of the low-pressure event. Vertical profiles of potential temperature (reference level at 1000 hPa) (d) before, (e) during, and (f) after the passage of the low-pressure. The stratification between the PBL and the lower atmosphere was weak during the low-pressure event.

During the cruise, SST (from the Thermosalinograph measurements) varied by less than 4°C (less than 1°C at the survey area) which had a negligible impact on the d-excess (+0.4‰/°C) [e.g., MJ79; *Majoube*, 1971]. Thereby in our study, atmospheric conditions are ideal to study the sensitivity of d-excess to relative humidity and wind speed in newly evaporated vapor.

3.2. Variability of the d-Excess

3.2.1. Sensitivity to Relative Humidity With Respect to the SST (Rhs)

In Figure 7, d-excess is plotted versus Rhs, the relative humidity reported at the sea surface temperature. The red points correspond to the measurements. The black line is the linear regression calculated from all the data and shows that d-excess is strongly negatively correlated with Rhs ($r^2 = 0.89$). The slope is −0.45‰/% and the closure equation leads to a slope of −0.43‰/% for smooth regime. In this region of high excess evaporation, the sensitivity of d-excess to Rhs is mostly well reproduced by the closure equation. The highest d-excess corresponds to the lowest Rhs leading to a stronger evaporation rate that increases kinetic processes [*Dansgaard*, 1964]. In 2008, Uemura et al. have measured isotopes of water vapor in the austral ocean during a month from 35°S to 65°S. In their study, the slope is −0.52‰/% and is comparable with the slope of −0.45‰/% from our data. In our study, SST variations had a negligible impact on the d-excess which could explain why the correlation coefficient between Rhs and d-excess is higher in our study ($r^2 = 0.89$) than in *Uemura et al.* [2008] study ($r^2 = 0.63$). Indeed in this last study, the much larger range of SST variations (≈ 23°C) explained a significant part of the d-excess variability ($r^2 = 0.55$).

3.2.2. Sensitivity to Surface Wind Speed

In addition to Rhs and SST, wind speed controls also d-excess (MJ79). During the rough regime (at the onset of wave breaking), the isotopic transport is mainly by turbulent diffusion, leading to low d-excess. Sea spray can be

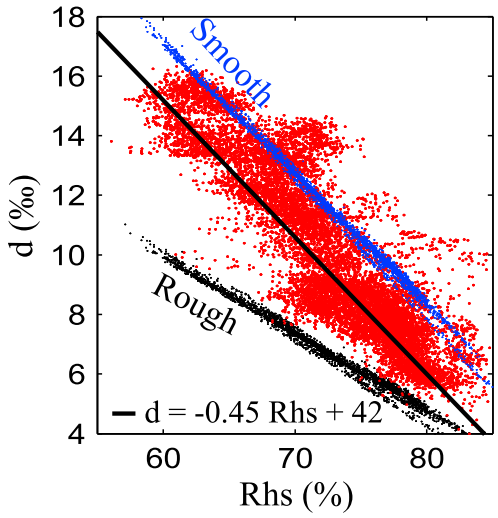

Figure 7. Correlations of d-excess in water vapor versus Rhs. The red points correspond to the measurements during the STRASSE cruise. The dark line represents a linear regression based on all the data ($d = -0.45\ \mathrm{Rhs} + 42$). The blue (black) points are d-excess calculated from the closure equation for the smooth (rough) regime.

produced during rough regime, and this process can also affect the d-excess. Conversely during the smooth regime, molecular diffusion controls mainly the isotopic transport leading to stronger kinetic process and higher d-excess [*Craig and Gordon*, 1965]. This dependence on wind speed has been established experimentally by MJ79, and we tried to check it with the in situ observations. In Figure 7, blue (black) points are the estimations from the closure assumption for the smooth (rough) regime. During the whole cruise, wind speed varied from 0 to 12 m s^{-1} thus exploring the two regimes for the ocean surface. Figure 7 indicates that most measurements fall within the boundaries corresponding to the two kinetic fractionation factors for smooth and rough regimes. As expected, d-excess from the rough regime is lower than for the smooth regime. The difference in d-excess between the two regimes is around 5‰ and increases when Rhs decreases. We also find that during large Rhs deficit, data are closer to the blue points corresponding to the smooth regime. This observation could result from the association of low wind speed conditions with lower Rhs (correlation coefficient $r^2 = 0.46$). Indeed, increased subsidence in the high-pressure system, leading to the transport of dry air from upper levels to the surface, is often associated with calm conditions, thus low wind speeds.

Figure 8 compares time series of d-excess from STRASSE measurements (black curve) with d-excess estimated from the closure assumption (orange and red curves). The orange (red) curve is d-excess calculated with kinetic fractionation factors for the smooth (rough) regime. During two periods (from 17 to 22 August and from 4 to 7 September, green shading in Figure 8), wind speed was particularly low, sometimes around 2 m s^{-1}. At this time, measurements agree well with the closure assumption using the kinetic fractionation for the smooth regime. Around 22 August 2012, the wind speed increased up to 7 m s^{-1} (corresponding to blue shading). Simultaneously, d-excess decreased quickly (in less than 12 h) to reach values calculated for the rough regime. This d-excess decrease of 5‰ can correspond to the transition from smooth regime to rough regime. During the next few days (from 24 to 31 August), wind speed remained high around 7 m s^{-1} and the measurement is between the two extreme values corresponding to different regimes. There was a change of wind direction during the transition on 22 August (see Figure 8). It is possible that the air mass seen after 22 August had witnessed the high winds before, and that its d-excess had already adjusted. This air mass change could explain why the d-excess decrease is faster than the time response of the water vapor into the boundary layer.

From 31 August to 2 September, d-excess reached the value for the smooth regime while wind speed reached 10 m s^{-1} between 31 August and 1 September. Then, the wind speed decreased and the maximum value of d-excess was found at the time of the minimum value of wind speed (3 m s^{-1} on the morning of 2 September). During this period (red shading in Figures 5 and 8), we know from radiosondes that a strong vertical mixing with the lower atmosphere happened (see Figure 6). On 1 September, a short event of rain occurred and cumulonimbus clouds were present in the late afternoon/evening. Moreover, this period is simultaneous with an important decrease in isotopic compositions of water vapor (2.5‰ for δ^{18}O and 18‰ for δD), in relative humidity (see Figure 5, red shading). During this event, it could have an isotopic exchange between falling rain and water vapor [*Bony et al.*, 2008]. There should also be a contribution to near surface water vapor from vertical mixing bringing humidity from the lower atmosphere in the PBL. Thus, this period should deviate from the closure assumption in MJ79, and the observed increase of d-excess would not be linked only to a wind speed decrease and could be also due to vertical mixing with tropospheric air. However, the increase of d-excess is reproduced by the closure equation and could be due to the increase of kinetic processes in response to the decrease of Rhs (10%). After the passage of the perturbation, the wind was again from the east with the wind regime controlled as before by trade winds and d-excess decreased abruptly. The

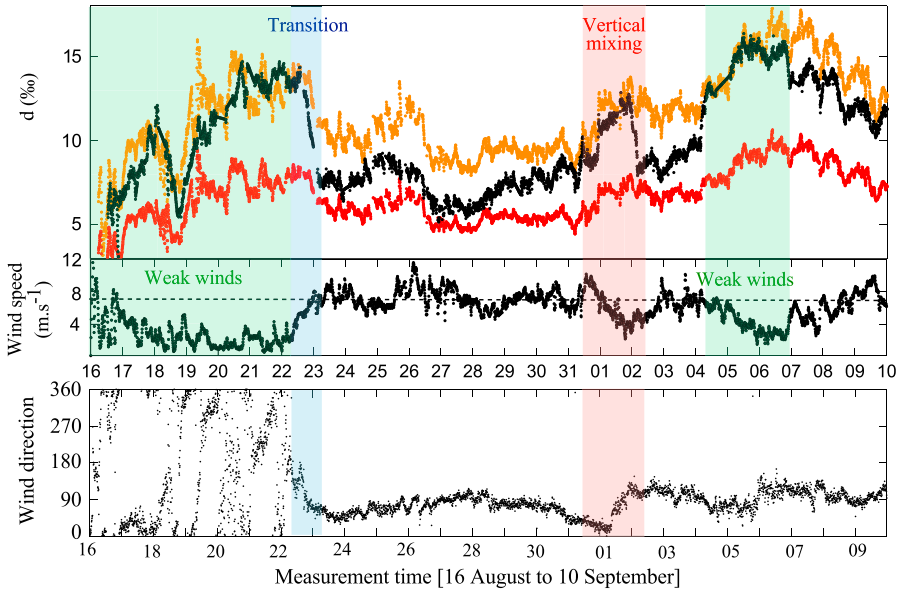

Figure 8. Variation of d-excess from 16 August to 10 September 2012. The black curve corresponds to measurements during the STRASSE cruise. The orange (red) curve is d-excess calculated with kinetic fractionation factor for smooth (rough) regime. The green shading is for the smooth regime and the blue shading is for a transition period. The red shading period corresponds to important vertical mixing with the lower troposphere. (middle) The wind speed corrected at 10 m. The dotted line corresponds to 7 m s^{-1}, the transition between smooth and rough regime. (bottom) The wind direction.

radiosondes indicated that the vertical mixing was over and during 2 days a stronger wind speed explains the lower d-excess. On 4 September, the d-excess increased to 14‰, although this increase is not clearly associated with a decrease of wind speed. Between 4 and 7 September (green shading in Figure 8), the wind weakened and stayed much lower than 7 m s^{-1}. The d-excess is thereby much closer to the d-excess calculated for the smooth regime. After that the wind speed increased and the measured d-excess decreased to be lower than the d-excess estimated for smooth regime.

These observations suggest that the use of the different kinetic fractionation factors as a function of wind speed can explain a part of the d-excess variability. Taking this into account can lead to variation of d-excess of 5‰. This data set is consistent with the range of kinetic fractionation factors estimated by MJ79. Nevertheless, we can note that during period of weak winds, the smooth regime corresponds closely to the observations, whereas during period of stronger winds, the extreme value of rough regime is approached but has never been reached. During the cruise, the smooth regime was dominant. The d-excess could result from an averaging between the extreme values of both regimes, in proportion to the dominance of one particular wind regime. Taking into account the evaporation rate and the thickness of the PBL, the response time of the isotopic composition and the d-excess in the PBL is on the order of a few days. The water vapor reservoir of the PBL is large and is not replaced instantaneously when there is a change of wind regime. Moreover, the difference could also be due to uncertainties in the parameterization of the equation leading to the calculation of α_k. We carried the same comparison of d-excess using the molecular diffusion coefficients chosen by *Cappa et al.* [2003]. During rough regime, d-excess is 1‰ higher compared to MJ79's coefficient and thus is closer to the measurement. For smooth regime, d-excess is 1.75‰ higher and overestimates the measurements during periods of low wind. This study supports the range of value predicted by MJ79 and *Cappa et al.* [2003].

3.3. Influence of the Free Troposphere

In the present study we have shown that the d-excess data fit well with a model assuming a closure assumption. However, the isotopic compositions measured at 20 m were slightly lower than the values predicted by the closure assumption (around 1.5‰ for δ^{18}O and 11‰ for δD), which indicates that the dilution with the air above the PBL is not negligible (Rha just above the PBL is around 40% from radiosondes). Furthermore, this contribution from the upper layer affects more δ^{18}O and δD than the d-excess and thus indicates that the d-excess must be more homogeneous in the upper layer than δ^{18}O and δD.

We note that in Kurita study [2013], the d-excess measured near the surface is higher than the d-excess estimated by the closure assumption. This result conflicts with ours and suggests higher d-excess in the free troposphere affecting the marine boundary layer in the area considered in *Kurita* [2013]. In agreement with *Jouzel and Koster* [1996], even if the closure equation is generally invalid in mid- or high-latitudes oceanic regions, the equation applied to d-excess is verified in this central part of the North Atlantic subtropics, where the ratio of evaporation over precipitation is larger than 1 and where the mixing processes with the lower atmosphere are weak.

4. Conclusion

During 25 days in summer in a region of high excess evaporation in the subtropical North Atlantic, d-excess above the ocean is well explained by the closure assumption, except during a short period of convection deepening the PBL. Thus, contrary to the isotopic composition, the d-excess at 20 m in this region is barely modified by other atmospheric processes. This is consistent with the assumption that a considerable source of humidity into the lower PBL is sea surface evaporation. Another assumption is that mixing processes affect not much the d-excess in the PBL, which is mainly controlled by kinetic processes during evaporation. We show that d-excess variability is correlated with both Rhs and wind speed. During the cruise, a 25% increase in Rhs caused a 10‰ decrease in d-excess, while a change in the wind regime is associated with a d-excess variation of 5‰. The use of the different kinetic fractionation factors of MJ79 reproduces in part d-excess variations. These results could be important for paleoclimatic studies because variations of d-excess in ice-core samples are interpreted as variations of evaporation parameters at the ocean surface such as relative humidity and SST. Here we suggest that there is also a dependency in wind speed. Moreover, the understanding of the isotopic fractionation sensitivity to sea surface regime could help model isotope compositions of water vapor and thus better constrain the hydrological cycle. Some of the difficulties of general circulation models to simulate d-excess [e.g., *Steen-Larsen et al*., 2011] could be in part attributed to their difficulties in representing surface winds.

Acknowledgments
We are grateful to Kadmiel Maseyk, Jerôme Demange, Aicha Naamar, Olivier Cattani, Guillaume Tremoy, Benedicte Minster, and Sonia Falourd for having shared their technical knowledge. We thank also Amaelle Landais and Olga Hernandez for their help and encouragement. Furthermore, we are grateful to the reviewers for their constructive comments.

References

Barkan, E., and B. Luz (2005), High precision measurements of $^{17}O/^{16}O$ and $^{18}O/^{16}O$ ratios in H_2O, *Rapid Commun. Mass Spectrom.*, *19*, 3737–3742, doi:10.1002/rcm.2250.

Bony, S., C. Risi, and F. Vimeux (2008), Influence of convective processes on the isotopic composition (δ18O and δD) of precipitation and water vapor in the tropics: 1. Radiative-convective equilibrium and Tropical Ocean–Global Atmosphere–Coupled Ocean-Atmosphere Response Experiment (TOGA-COARE) simulations, *J. Geophys. Res.*, *113*, D19305, doi:10.1029/2008JD009942.

Cappa, C. D., M. B. Hendricks, D. J. DePaolo, and R. C. Cohen (2003), Isotopic fractionation of water during evaporation, *J. Geophys. Res.*, *108*(D16), 4525, doi:10.1029/2003JD003597.

Craig, H., and L. I. Gordon (1965), Deuterium and oxygen 18 variations in the ocean and marine atmosphere, in *Proceedings of a Conference on Stable Isotopes in Oceanographic Studies and Paleotemperatures*, edited by E. Tongiorgi, pp. 9–130, Lab. Geol. Nucl, Pisa, Italy.

Dansgaard, W. (1964), Stable isotopes in precipitation, *Tellus*, *16*, 436–468, doi:10.1111/j.2153-3490.1964.tb00181.x.

Gaillard, F., E. Autret, V. Thierry, P. Galaup, C. Coatanoan, and T. Loubrieu (2009), Quality control of large Argo datasets, *J. Atmos. Oceanic Technol.*, *26*(2), 337–351, doi:10.1175/2008JTECHO552.1.

Gat, J. R. (1996), Oxygen and hydrogen isotopes in the hydrologic cycle, *Annu. Rev. Earth Planet. Sci.*, *24*, 225–262.

Gat, J. R., B. Klein, Y. Kushnir, W. Roether, H. Wernli, R. Yam, and A. Shemesh (2003), Isotope composition of air moisture over the Mediterranean Sea: An index of the air–sea interaction pattern, *Tellus, Ser. B*, *55*, 953–965.

Horita, J., and D. J. Wesolowski (1994), Liquid-vapor fractionation of oxygen and hydrogen isotopes of water from the freezing to the critical temperature, *Geochim. Cosmochim. Acta*, *58*, 3425–3437, doi:10.1016/0016-7037(94)90096-5.

Jouzel, J., L. Merlivat, and C. Lorius (1982), Deuterium excess in an East Antarctic ice core suggests higher relative humidity at the oceanic surface during the last glacial maximum, *Nature*, *299*(5885), 688–691, doi:10.1038/299688a0.

Jouzel, J., and R. D. Koster (1996), A reconsideration of the initial conditions used for stable water isotope models, *J. Geophys. Res.*, *101*, 22,933–22,938, doi:10.1029/96JD02362.

Kurita, N. (2011), Origin of Arctic water vapor during the ice-growth season, *Geophys. Res. Lett.*, *38*, L02709, doi:10.1029/2010GL046064.

Kurita, N. (2013), Water isotopic variability in response to mesoscale convective system over the tropical ocean, *J. Geophys. Res. Atmos.*, *118*, 10,376–10,390, doi:10.1002/jgrd.50754.

Kurita, N., D. Noone, C. Risi, G. A. Schmidt, H. Yamada, and K. Yoneyama (2011), Intraseasonal isotopic variation associated with the Madden-Julian Oscillation, *J. Geophys. Res.*, *116*, D24101, doi:10.1029/2010JD015209.

Lawrence, J. R., S. D. Gedzelman, D. Dexheimer, H.-K. Cho, G. D. Carrie, R. Gasparini, C. R. Anderson, K. P. Bowman, and M. I. Biggerstaff (2004), Stable isotopic composition of water vapor in the tropics, *J. Geophys. Res.*, *109*, D06115, doi:10.1029/2003JD004046.

Luz, B., E. Barkan, R. Yam, and A. Shemesh (2009), Fractionation of oxygen and hydrogen isotopes in evaporating water, *Geochimica et Cosmochimica Acta*, *73*(22), 6697–6703, doi:10.1016/j.gca.2009.08.008.

Majoube, M. (1971), Fractionnement en oxygene-18 et en deuterium entre l'eau et sa vapeur, *J. Chim. Phys.*, *68*, 1423–1436.

Merlivat, L. (1978), Molecular diffusivities of $H_2{}^{16}O$, $HD^{16}O$, and $H_2{}^{18}O$ in gases, *J. Chem. Phys.*, *69*, 2,864–2,871, doi:10.1063/1.436884.

Merlivat, L., and J. Jouzel (1979), Global climatic interpretation of the deuterium-oxygen 18 relationship for precipitation, *J. Geophys. Res.*, *84*, 5029–5033, doi:10.1029/JC084iC08p05029.

Schmidt, M., K. Maseyk, C. Lett, P. Biron, P. Richard, T. Bariac, and U. Seibt (2010), Concentration effects on laser-based $\delta^{18}O$ and $\delta^{2}H$ measurements and implications for the calibration of vapour measurements with liquid standards, *Rapid Commun. Mass Spectrom.*, *24*(24), 3553–3561, doi:10.1002/rcm.4813.

Steen-Larsen, H. C., et al. (2011), Understanding the climatic signal in the water stable isotope records from the NEEM shallow firn/ice cores in northwest Greenland, *J. Geophys. Res.*, *116*, D06108, doi:10.1029/2010JD014311.

Steen-Larsen, H. C., et al. (2013), Continuous monitoring of summer surface water vapor isotopic composition above the Greenland Ice Sheet, *Atmos. Chem. Phys.*, *13*(9), 4815, doi:10.5194/acp-13-4815-2013.

Tremoy, G., F. Vimeux, O. Cattani, S. Mayaki, I. Souley, and G. Favreau (2011), Measurements of water vapor isotope ratios with wavelength-scanned cavity ring-down spectroscopy technology: New insights and important caveats for deuterium excess measurements in tropical areas in comparison with isotope-ratio mass spectrometry, *Rapid Commun. Mass Spectrom.*, *25*(23), 3469–3480, doi:10.1002/rcm.5252.

Tremoy, G., F. Vimeux, S. Mayaki, I. Souley, O. Cattani, C. Risi, G. Favreau, and M. Oi (2012), A 1-year long $\delta^{18}O$ record of water vapor in Niamey (Niger) reveals insightful atmospheric processes at different timescales, *Geophys. Res. Lett.*, *39*, L08805, doi:10.1029/2012GL051298.

Uemura, R., Y. Matsui, K. Yoshimura, H. Motoyama, and N. Yoshida (2008), Evidence of deuterium excess in water vapor as an indicator of ocean surface conditions, *J. Geophys. Res.*, *113*, D19114, doi:10.1029/2008JD010209.

Wüst, G. (1922), Evaporation and precipitation on the earth.1, *Mon. Weather Rev.*, *50*, 313–314, doi:10.1175/1520-0493(1922)50<313c.